Molecular Pharmacology Fast Forward. Published on July 12, 2007 as doi: 10.1124/mol.107.036939

The Endocannabinoid Anandamide Inhibits the Function of α4β2 Nicotinic Acetylcholine Receptors

Charles E. Spivak, Carl R. Lupica, and Murat Oz

United States Department of Health and Human Services, National Institutes of Health, National Institute on Drug Abuse, Intramural Research Program, Cellular Neurobiology Branch, Electrophysiology Research Unit, Baltimore, Maryland 21224, USA.

Molecular Pharmacology Fast Forward. Published on July 12, 2007 as DOI: 10.1124/mol.107.036939
This article has not been copyedited and formatted. The final version may differ from this version.

Running title: Anandamide inhibits α4β2 nicotinic receptors

Corresponding author: Charles Spivak

National Institute on Drug Abuse, Intramural Research Program

Cellular Neurobiology Branch, Electrophysiology Unit

5500 Nathan Shock Drive

Baltimore, Maryland 21224, USA.

Number of text pages:	32
Number of tables:	0
Number of figures:	8
Number of words in abstract:	245
Number of words in Introduction:	335
Number of words in Discussion:	1809

ABBREVIATIONS: ACh, acetycholine; AEA, arachidonylethanolamide, anandamide, N-(2-hydroxyethyl)-5,8,11,14-eicosatetraenamide (all-Z)-; BAPTA, 1,2-bis(2-aminophenoxy)ethane-N,N,N',N'-tetraacetic acid; BSA, bovine serum albumin; CB1, cannabinoid type 1 receptor; EGTA, ethylene glycol-bis(2-aminoethylether)-N,N,N',N'-tetraacetic acid; FAAH, fatty acid amide hydrolase; 5-HT_3, 5-hydroxytryptamine type 3 receptor; nAChR, nicotinic acetylcholine receptor; NMDA, N-methyl-D-aspartic acid; SR-141716A, 5-(4-chlorophenyl)-1-(2,4-dichlorophenyl)-4-methyl-N-(piperidin-1-yl)-1H-pyrazole-3-carboxamide; (Δ^9-THC , Δ^9-tetrahydrocannabinol; URB 597, cyclohexyl carbamic acid 3'-carbamoylbiphenyl-3-yl ester.

Molecular Pharmacology Fast Forward. Published on July 12, 2007 as DOI: 10.1124/mol.107.036939
This article has not been copyedited and formatted. The final version may differ from this version.

ABSTRACT

The effects of the endocannabinoid anandamide (arachidonylethanolamide, AEA) on the function of α4β2 nicotinic acetylcholine receptors (nAChR) stably expressed in SH-EP1 cells were investigated using the whole-cell patch clamp technique. In the concentration range of 200 nM to 2 μM, AEA significantly reduced the maximal amplitudes and increased the desensitization of ACh-induced currents. The effects of AEA could be neither replicated by the exogenous cannabinoid Δ^9-tetrahydrocannabinol (Δ^9-THC, 1 μM), nor reversed by the selective CB1 receptor antagonist SR-141716A (1 μM). The actions of AEA were apparent when applied extracellularly, but not during intracellular dialysis. Furthermore, the effects of AEA on ACh currents were not altered by the calcium chelator BAPTA. The onset and washout of the AEA effects required several minutes (10-30 min), but the latter was significantly decreased in the presence of lipid free bovine serum albumin (BSA). Moreover, BSA alone increased peak ACh current amplitudes and diminished desensitization rates in naïve cells, suggesting a tonic modulation of α4β2 nAChR function by an endogenous AEA-like lipid. Further analysis of AEA effects on α4β2 nAChR mediated currents, using a two-stage desensitization model, indicated that the first forward rate constant leading to desensitization, k_1, increased nearly 30-fold as a linear function of the AEA concentration. In contrast, the observation that the other three rate constants were unaltered by AEA suggested that AEA raised the energy of the activated state. These results indicate that AEA directly inhibits the function of α4β2 nAChRs in a CB1-receptor independent manner.

Molecular Pharmacology Fast Forward. Published on July 12, 2007 as DOI: 10.1124/mol.107.036939
This article has not been copyedited and formatted. The final version may differ from this version.

INTRODUCTION

Arachidonylethanolamide is an endogenously produced fatty acid ethanolamide that activates cannabinoid receptors to produce cellular and pharmacological effects similar to Δ^9-THC, the psychoactive component of marijuana (for reviews Howlett et al. 2002; Pacher et al., 2006). However, several reports indicate that AEA can produce effects that are not mediated by the activation of the cloned CB_1 or CB_2 receptors. For example, it has been demonstrated that AEA inhibits the functions of voltage-dependent-Ca^{2+} channels (Oz et al., 2000; Chemin et al., 2001), Na^+ channels (Nicholson et al., 2003), various types of K^+ channels (Poling et al., 1996; Oliver, 2004), 5-HT_3 receptor function (Barann et al., 2002; Oz et al., 2002a), and nicotinic ACh receptors (Oz et al., 2003) in a cannabinoid receptor-independent manner (for a review Oz ., 2006). These findings can suggest that additional molecular targets for AEA exist in the CNS.

The nAChR containing α4β2 subunits, the predominant subtype in the CNS, has been linked to the positive-reinforcing and cognitive effects of nicotine (Tapper et al., 2004; Brody et al., 2006), and its high affinity for nicotine has lead to the proposal that it is a primary target for nicotine's actions in the CNS (Laviolette and van der Kooy, 2004). In support of this view, recent studies with mutant mice demonstrated that the α4β2 nAChR was necessary to observe tolerance and sensitization to nicotine *in vivo* (Tapper et al., 2004). Biochemical, electrophysiological, behavioral, and clinical evidence support the existence of functional interactions between nicotinic receptors and cannabinoids, including AEA (for reviews Castane et al., 2006; Viveros et al., 2006). In addition, we have shown that the endogenous cannabinoid AEA inhibits ion currents

Molecular Pharmacology Fast Forward. Published on July 12, 2007 as DOI: 10.1124/mol.107.036939
This article has not been copyedited and formatted. The final version may differ from this version.

mediated by the activation of nACh α_7 receptors expressed in *Xenopus* oocytes (Oz et al., 2003).

To date, the functional interaction between α4β2 nAChR and cannabinoid receptor ligands such as AEA and Δ^9-THC has not been investigated. In the present study, we examine the effects of these cannabinoids on the function of α4β2 nAChR receptors stably transfected in the SH-EP1 cell line.

Molecular Pharmacology Fast Forward. Published on July 12, 2007 as DOI: 10.1124/mol.107.036939
This article has not been copyedited and formatted. The final version may differ from this version.

MATERIALS AND METHODS

Cell Culture

The SH-EP1 cells stably expressing the human α4β2 nAChR, a gift from Dr. R Lukas (Barrow Neurological Institute, Phoenix, AZ), are described elsewhere (Pacheco et al., 2001). They were grown on 35 mm dishes in DMEM (Gibco, Gaithersberg, MD) supplemented with 10% heat inactivated horse serum (Gibco), 5% fetal bovine serum (Gibco), 1 mM sodium pyruvate, 100 U/mL penicillin G, 100 μg/mL streptomycin, 0.25 μg/mL amphotericin B, 0.4 mg/mL hygromycin B, and 0.25 mg/mL Zeocin (Gibco). The cells were maintained at 37^{o} C in an atmosphere of 5% CO_2 saturated with H_2O.

Electrophysiological Recording

The cells were recorded at ambient temperature while superfused at 2.0 mL/min with Dulbecco's phosphate buffered saline augmented with sucrose to match the osmolarity (340 mOsm) of the growth medium. The composition was (in mM): NaCl, 136.9; KCl, 2.68; $MgCl_2$, 0.49; $CaCl_2$, 0.9; KH_2PO_4, 1.47; Na_2HPO_4, 8.1, glucose, 5.55; sucrose, 45.0; pH 7.40. The intracellular solution contained in the patch pipettes was modified to minimize ACh current rundown (Wu et al., 2004), and consisted of (in mM): TRIS phosphate dibasic, 110; TRIS base, 28; $MgCl_2$, 2; $CaCl_2$, 0.1; EGTA, 11; $Mg_3(ATP)_2$, 1.8; brought to pH 7.30 with H_3PO_4. Because this pipette medium has about 40% of the specific conductance of a corresponding KCl solution, open pipettes had resistances of 4 – 8 MΩ despite having tip diameters of about 1.5 μm. Conventional whole cell recording conditions were established after first achieving a 1 - 5 GΩ cell-

attached seal. The cells were voltage clamped at -60 mV using an Alembic VE-2 whole cell amplifier (Alembic Instruments, Montreal, Canada). Series resistance, measured using a 10 mV step before each test, was 100% compensated. Drugs were locally superfused using a modified U-tube (Murase et al., 1989) positioned 35 μm above and 190 μm lateral to the base of the patch-clamped cell. Local superfusion with 150 mM choline chloride in this configuration demonstrated a change in junction potential at an open tipped pipette with a 10 - 90% rise times of 2 to 3 ms. This time sets the lower limit of cellular rise times to ACh application. Acetylcholine was applied to voltage clamped cells for 4.9 s at 30 μM unless noted otherwise. The currents, recorded using pClamp 7.0 software (Axon Instruments Inc., Union City, CA), were filtered (low pass) to 200 Hz and sampled at 1 kHz. The cells generally had ~ 30 pF capacitance and 60 - 150 MΩ membrane resistance. Data means ± s.e.m. were compiled from three to six cells.

Acetylcholine was used as the agonist to probe receptor function. We preferred it over other agonists mostly because of its low hydrophobicity, making it easy to wash out, and because, unlike nicotine, it has limited ability to desensitize the α4β2 nAChRs (Paradiso and Steinbach, 2003). Acetylcholine (Sigma, St. Louis, MO) was diluted each day from a 10 mM stock that was prepared weekly. AEA (Tocris Bioscience, Ellisville, MO) was diluted daily from a stock solution prepared in ethanol (14.4 mM) stored at -20^{o} C and dispensed directly into the superfusion solution. SR-141716A and Δ^{9}-THC were obtained from the NIDA Drug Supply System (Bethesda, MD).

Molecular Pharmacology Fast Forward. Published on July 12, 2007 as DOI: 10.1124/mol.107.036939
This article has not been copyedited and formatted. The final version may differ from this version.

Data analysis

Average values were calculated as mean ± standard error of the mean (s.e.m.). Statistical significance was evaluated using Student's *t* test. Concentration-response parameters were obtained by fitting the data to the logistic equation,

$$y = E_{max}/(1+[x/EC_{50}]^n),$$

where x and y are concentration and response, respectively, E_{max} is the maximal response, EC_{50} is the half-maximal concentration, and n is the slope factor (apparent Hill coefficient). For data analysis and calculations of concentration response curve data, we used the computer program MLAB (Civilized Software, Bethesda, MD).

The kinetic analyses of the current decays were performed using the modeling program MLAB. A more intuitive explanation is given in the supplementary materials. The kinetic analysis incorporated only the decay phases of the responses because the kinetics of the rising phases were limited by various parameters including the cell size, the unstirred layer (Spivak et al., 2006) and the perfusion rate (see supplementary materials). The decay phase was modeled as a two-stage sequential desensitization process:

[INSERT SCHEME 1 HERE]

where AR* represents the activated (open channel) state, AR the first desensitized state, and AR the second desensitized state. It was assumed that at the peak of the response, AR' = AR" = 0. The parameters AR* (initial), k_1, k_{-1}, k_2, and k_{-2} were fitted simultaneously by nonlinear regression analysis to each decay.

Molecular Pharmacology Fast Forward. Published on July 12, 2007 as DOI: 10.1124/mol.107.036939
This article has not been copyedited and formatted. The final version may differ from this version.

RESULTS

Acetylcholine Concentration Response

ACh-induced inward currents were elicited using various concentrations of the agonist at a fixed treatment time of 4.9 s, and delivered in random order to voltage clamped cells (Fig. 1). These currents were mediated by the nAChR, as these cells are devoid of muscarinic receptors (Lambert et al., 1989). ACh application evoked an inward current whose amplitude was dependent upon its concentration. A maximal activation of this current was seen at approximately 100 μM ACh, and the EC_{50} was 40 ± 5 μM. Rise times (10 - 90%) for the ACh-evoked currents were < 100 ms, and typically about 50 ms, which was about 20-times greater than the time required for solution change (see Materials and Methods). The responses usually decayed as double exponential functions of time, reflecting two phases of desensitization (see Materials and Methods). At low ACh concentrations, double exponential decays became difficult or impossible to discern from single exponentials because the signal was smaller and because k_1 appoached k_2 (Fig. 2A and 2C). As a result, parameters for the second stage of desensitization were more prone to error or were impossible to obtain (such as the k_2 and k_{-2} values for 1 μM ACh in Fig. 2). Figure 2 depicts the relationships between the fitted rate constants to the ACh concentration. The rate constant k_1 increased about 16-fold as a function of the ACh concentration (1 to 1000 μM; Fig. 2A) and was directly proportional to the activated state AR* (Fig. 2B), as required by the desensitization scheme. In contrast, k_2 showed only a slight tendency to increase with the ACh concentration (Fig. 2C) with no correlation to the activated state (Fig. 2D). The backward rate constants, k_{-1}

Molecular Pharmacology Fast Forward. Published on July 12, 2007 as DOI: 10.1124/mol.107.036939
This article has not been copyedited and formatted. The final version may differ from this version.

and $k_{-2,}$ showed no change with ACh concentration (Figs. 2E and 2F). These relationships are consistent with the desensitization scheme above.

Effects of AEA on α4β2 nAChR kinetics

Figure 3A illustrates the three features of the AEA effect on ACh responses: (1) a decrease in peak amplitude, (2) an increase in the decay rate of the more rapid phase of the response, and (3) that these effects increase gradually over tens of minutes. The declines of peak amplitude are summarized in Fig. 3B, which shows that the progressive decrease in normalized peak amplitudes required at least 20 minutes of exposure to AEA and increased with the AEA concentration. Exponential time constants are 12.2, 12.2, 6.1, and 4.4 min for AEA concentrations of 0.2, 0.5, 1, and 2 μM, respectively. From inspection of Fig. 3B one obtains an estimate of IC50 (at 20 min) of about 300 nM. AEA concentrations higher than 2 μM were not systematically tested because the ACh currents were completely inhibited.

The decays of the ACh-induced currents in the presence of AEA were fitted to the desensitization scheme given above to derive the four rate constants. Figure 3C shows that the values of the first forward rate constant for desensitization k_1, determined for AEA concentrations up to 2 μM increased as exponential functions of time, and their asymptotic maxima increased as linear functions of the AEA concentration (Fig. 3D) with no sign of saturation. In contrast, the estimates of all of the remaining rate constants were independent of time and insensitive to AEA (Fig. 3 E-G).

Molecular Pharmacology Fast Forward. Published on July 12, 2007 as DOI: 10.1124/mol.107.036939
This article has not been copyedited and formatted. The final version may differ from this version.

We next investigated whether cannabinoid receptors were involved in the inhibitory effects of AEA on α4β2 nAChR function, or whether there were also direct effects of other cannabinoid ligands on this nAChR. The primary psychoactive constituent of cannabis, Δ^9-THC (1 μM), did not alter the amplitudes or the kinetics of the current elicited by ACh (Fig. 4). In addition, the cannabinoid receptor antagonist SR-141716A (rimonabant), which had no effect by itself on ACh responses (n=3), did not significantly alter the effects of AEA on the α4β2 nAChR (Fig. 5A, C, D, and E). However, SR-141716A did seem to reverse slightly the effect of AEA on rate constant k_1 (Fig. 5B).

The site of the AEA action was further tested by including the endocannabinoid (1 μM) in the pipette solution. To prevent possible hydrolysis of AEA to arachidonic acid by fatty acid amide hydrolase (FAAH), 1 μM URB 597, the specific and potent FAAH inhibitor (Kathuria et al., 2003) was included in the patch pipette. Application of ACh at 3 min intervals for up to 40 min showed a rundown of peak amplitudes to 80 ± 11% (n=6), which was indistinguishable from the control value of 88 ± 5% (n=4; $P > 0.5$). In addition, the value of the first forward rate constant for desensitization, k_1 increased slightly from 1.52 ± 0.34 s^{-1} to 1.96 ± 0.61 s^{-1} at 30 min (n=6), values that are in complete agreement with controls ($P > 0.4$) and in striking contrast to the effects of 1 μM AEA applied extracellularly (Fig. 3C). These results require more thorough study, however, because hydrophobic compounds may not be efficiently delivered by means of a patch pipette (Akk et al., 2005).

In earlier studies, AEA has been shown to increase intracellular Ca^{2+} levels (for review Oz, 2006). Furthermore, the α4β2 nAChR is permeable to Ca^{2+} (for a review

Molecular Pharmacology Fast Forward. Published on July 12, 2007 as DOI: 10.1124/mol.107.036939
This article has not been copyedited and formatted. The final version may differ from this version.

Fucile, 2004), and various second messenger cascades activated by increased levels of intracellular Ca^{2+} could modulate the function of these receptors and mimic the actions of AEA. For this reason, we tested the effect of the high affinity, fast acting calcium chelator BAPTA on AEA inhibition of the α4β2 nAChR. However, inclusion of BAPTA (11 mM) in the pipette solution did not alter the effects of extracellular AEA on the peak amplitudes and desensitization rates of the α4β2 nAChR-mediated currents. Thus, after 30 min of 1 μM AEA treatment, peak amplitudes for BAPTA vs. control were 10.8 ± 4.1 (n=3) and 13.0 ± 3.7 (n=3) percent of the initial values, respectively ($P > 0.3$). The corresponding values of k_1 were 19.0 ± 4.3 s^{-1} (n=3) and 25.3 ± 5.2 s^{-1} (n=4), respectively ($P > 0.4$). To avoid the possibility of any local rise in unbuffered Ca^{2+} concentration, we replaced calcium with equimolar barium in the extracellular medium and tested the effects of 0.5 μM AEA on 30 μM ACh responses. On comparing the results to those obtained in calcium-containing medium, we found no change in peak amplitudes and rate constants k_{-1}, k_2, and k_{-2} (4 or 5 cells, monitored for 40 min). The rate constant k_1, however, was 61 ± 3% of the corresponding value in calcium-containing medium for all time points including those before the application of AEA. Because of the constant percent decrease of k_1 on the cells even before AEA treatment, we believe that the barium-containing medium, rather than antagonizing AEA directly, lowered the free energy of the activated state, and that the barium and AEA effects were independent and additive.

An open-channel blockade, by definition, requires the opening of the channel by the binding of agonist to the receptor. Thus, in the absence of an agonist, pretreatment with a blocker should not cause inhibition, and the degree of blockade should be related

to the frequency of channel activation. Therefore, the extent of AEA inhibition of the α4β2 nAChR-mediated response was compared in cells exposed to ACh at 6 min intervals with those exposed at 3 min intervals. However, increasing the ACh test interval to 6 minutes during AEA (1 μM) application gave responses indistinguishable from those tested at the 3 min interval, indicating that the block by AEA was not use dependent (Fig. 3B).

If the slow onset of the AEA effects was a consequence of its partitioning into the lipid membrane, then the time course of reversal of the AEA effect should be similar to onset during simple washout, but greatly enhanced if a lipid scavenger is included in the extracellular solution. The offset kinetics were first tested under normal conditions (Fig. 6 A and B). Because our objective was to characterize the reversal of the AEA treatment by monitoring this phase as long as possible, we applied the endocannabinoid for only 3 min prior to beginning the wash phase. This application period is seen in Fig. 6 A and B as the gap between the last control test and the first test after beginning the wash period denoted by the pair of dotted vertical lines. The peak ACh-induced current amplitudes were reduced to 60% of control by this application of AEA and intersected the control rundown curve at about 50 min after the start of the wash (Fig 6A; the dashed line, taken from Fig. 3B). The recovery of the k_1 values were clearer, approaching the control value during the wash phase as an exponential function of time with a time constant of 30 ± 4 min (Fig. 6B). In the next series of experiments, we recorded control responses to ACh in BSA-free medium. The cells were then treated with 1 μM AEA for 10 min followed by a wash with 1 mg/mL of lipid free BSA (e.g. Poling et al., 1996). Figures 6C and 6D reveal that the recovery of peak amplitudes and k_1 were complete by 9 min, an order of

Molecular Pharmacology Fast Forward. Published on July 12, 2007 as DOI: 10.1124/mol.107.036939
This article has not been copyedited and formatted. The final version may differ from this version.

magnitude faster than recovery without BSA (the time constants were 2.2 and 1.7 min, respectively). In addition, the amplitudes of the ACh-evoked currents during BSA treatment appeared to be larger than those observed during the control baseline period, observed prior to AEA application (Fig 6C). We speculated that this might result from the tonic inhibition of the α4β2 nAChR by an endogenous lipid molecule that was sensitive to BSA. To test this hypothesis, we examined the effects of BSA on ACh-evoked currents in the absence of AEA application (Fig. 7). Treatment with BSA alone (14 min) caused significant effects on peak amplitudes of the α4β2 nAChR currents as well as the rate constant k_1 that were opposite to those caused by AEA. Furthermore the effects of BSA were reversible by a brief washing with control saline. BSA had no effects on the other rate constants.

Molecular Pharmacology Fast Forward. Published on July 12, 2007 as DOI: 10.1124/mol.107.036939
This article has not been copyedited and formatted. The final version may differ from this version.

DISCUSSION

The present results indicate that the endocannabinoid AEA inhibited the function of the α4β2 nAChR in a cannabinoid receptor-independent manner. Furthermore, this effect was relatively selective for this cannabinoid receptor agonist because the phytochemical agonist Δ^9-THC was ineffective in modulating nAChR-mediated ion currents, and the cannabinoid antagonist SR-141716A did not affect the AEA inhibition of α4β2 nAChR function. These results therefore indicate that AEA acts directly at the α4β2 nAChR independently of cannabinoid receptors to modulate the strength of nicotinic signaling. In agreement with these results, AEA has also been found to modulate the functions of other voltage-gated (Poling et al., 1996; Oz et al., 2000; Oliver et al., 2004; Fisyunov et al., 2006) and ligand-gated (Barann et al., 2002; Oz et al., 2002; 2003; 2004a) ion channels, as well as other integral membrane proteins at a similar concentration range and in a cannabinoid-receptor independent manner (for a review see Oz, 2006).

The α4β2 nAChR is highly permeable to Ca^{2+} (for a review, Fucile, 2004), and the nAChR-induced increases in intracellular Ca^{2+} levels can activate various second messengers that modulate the function of the receptors in a feedback fashion (e.g. Fenster et al., 1999). However, in the present work, the inclusion of BAPTA in the pipette solution and the replacement of extracellular Ca^{2+} with Ba^{2+} did not alter the AEA inhibition of the α4β2 nAChR, suggesting that the changes in the intracellular Ca^{2+} levels were not involved in AEA actions on these receptors. In other studies, the ability of AEA to inhibit the function of ion channels (reviewed in Oz, 2006) has been ascribed to an action at an intracellular binding site. To test this hypothesis, we dialyzed the cell with

Molecular Pharmacology Fast Forward. Published on July 12, 2007 as DOI: 10.1124/mol.107.036939
This article has not been copyedited and formatted. The final version may differ from this version.

AEA in the pipette, ACh produced currents with amplitudes and decay kinetics that were indistinguishable from controls, suggesting that the site of AEA action was extracellular. However, given the rapid traverse of fatty acids across phospholipid membranes (e.g. Kamp and Hamilton, 1993) and the caution required in interpreting intracellular application of hydrophobic substances (Akk et al., 2005), we view the site of AEA action as inconclusive.

In agreement with earlier findings (e.g. Paradiso and Steinbach, 2003; Wu et al., 2004), α4β2 nAChR currents in voltage clamped SH-EP1 cells decayed with double exponential kinetics, which can be analyzed as two mechanistic states of desensitization (Scheme 1). Though a simplification of comprehensive schemes (e.g. Paradiso and Steinbach, 2003; Quick and Lester, 2002), Scheme 1 was useful because it accounted for the data by ascribing a mechanism to the decays in the ACh currents, both alone and in the presence of AEA Thus, the rate constant k_1, which leads from the activated to the first desensitized state, was found to be a function of the ACh concentration (Fig. 1A) and was directly proportional to the activated state (AChR* of Scheme 1) of the nAChR (Fig. 1B), whereas the other rate constants were independent of these variables (Fig. 1C-1F). Therefore, this model parsimoniously described our data while providing mechanistic insight into the desensitization of the $\alpha_4\beta_2$-nAChR by AEA. The most striking effect of AEA in this model was the linear increase in the value of k_1 with increasing AEA concentrations, such that at 2 μM AEA it was 27-fold higher than the control value. The other rate constants remained unchanged by AEA. This selectivity can be understood in terms of energy states of the α4β2 nAChR. If the activation energy barrier between the activated (AChR*) and the first desensitized state (AChR'; Scheme

Molecular Pharmacology Fast Forward. Published on July 12, 2007 as DOI: 10.1124/mol.107.036939
This article has not been copyedited and formatted. The final version may differ from this version.

1) were lowered by AEA (Fig. 8, dotted line), then both k_1 and k_{-1} would have increased. However, if AEA increased the energy of the activated state AR* (Fig. 8, dashed curve), then only k_1 would increase, as observed. This explanation implies that AEA will cause a faster closure rate of the open ion channel and hence a reduction in peak amplitudes due to a lower open probability of the ion channel. These predictions are testable by single channel recording experiments that are currently in progress.

Open channel blockade is the most widely used model to describe the block of ligand-gated ion channels. However, this model is inappropriate to describe the present data for the following reasons: (1) Under conditions of low free concentrations of a blocking ligand, such as AEA, no occlusion should occur. Therefore, in the present data the scavenging of free AEA by BSA should be especially effective in preventing open channel blockade, but three min after BSA treatment the decay (expressed as k_1) was still accelerated (Fig. 6D). (2) There was an absence of use-dependent blockade (Fig. 3B), and AEA had almost no effect when co-administered with ACh without preincubation (data not shown). Open channel blockade could occur in the absence of AEA in free solution if AEA first dissolved into the lipid membrane and diffused into a non-annular lipid space to block the ion channel. Scheme 1, validated by the ACh concentration response curves, would then be enlarged by adding a second pathway from the activated to the blocked state. Because this model predicted alterations in all four parameters that we did not observe, we therefore conclude that Scheme 1 remains the most parsimonious and useful model for the data.

The striking decrease in the peak amplitudes seen in the presence of AEA could be a consequence of the increase in the rate of desensitization (k_1), as described in our

Molecular Pharmacology Fast Forward. Published on July 12, 2007 as DOI: 10.1124/mol.107.036939
This article has not been copyedited and formatted. The final version may differ from this version.

model. It is important to understand that, whereas the fastest perfusion-limited rise time that can be observed in our system is the 2-3 ms rise time of the junction potential occurring with a solution change, the rise time for the ACh currents was ~40 ms. This discrepancy likely reflects the time required for ACh to diffuse through the unstirred layer of extracellular solution that surrounds cultured cells under the present conditions. A similar kinetic slowing of the effects of the opioid antagonist naloxone (Spivak et al., 2006) and AEA (Bojesen and Hansen, 2006) by the unstirred layer have also recently been described. In the presence of AEA, this may have led to a desensitization gradient across the cell in which nAChRs in regions of the cell membrane that were activated first by ACh, desensitized before more distal nAChRs were activated. Simulations (see supplemental information) that convolve this diffusion of ACh through the unstirred layer with α4β2 nAChR desensitization show that about 80% of the decrease in response amplitude can be attributed to this mechanism. A consistent and parsimonious explanation for the remainder of the decrease is to ascribe it to desensitization of the nAChR in the closed state, a process supported by previous work of others and which seems particularly important for the agonist nicotine (Paradiso and Steinbach, 2003)

Another result of the kinetic analysis was that the increase in k_1 showed no sign of approaching saturation over the entire effective range of AEA concentrations (Fig. 3D). This is consistent with our molecular view of the effect of AEA on ion channels. Given an estimated octanol-water partition coefficient of $1.7x10^5$ (Log P from ChemDraw, CambridgeSoft, Cambridge MA), it is likely that AEA will easily partition into the biological membrane, where it can rapidly displace some of the ~40 annular (Ellena et al., 1983) and possibly the non-annular lipids that are in intimate contact with the receptor.

Such alterations of the lipid environment, which include hydrophobic mismatch between lipids and proteins, changes in membrane viscosity, changes in the interfacial curvature, altered lateral pressure profile, and shifts in lipid dipole potential and surface potential can alter the functions of transmembrane proteins (e.g. Barrantes, 2004; Lundbaek, 2006). Specifically, we propose that AEA has raised the free energy of the activated state AR*.

Anandamide belongs to a larger group of signaling lipids consisting of amides of long-chain polyunsaturated fatty acids (for a review see Howlett et al., 2002). Earlier studies on nAChRs demonstrated that fatty acids could modulate their function via a direct action (for a review see Barrantes, 2004). Thus it is possible that AEA and fatty acid based molecules may share common sites of action on various membrane proteins (for a review see Oz, 2006). Depending upon local concentrations under basal conditions, the modulatory actions of AEA on nAChRs might be tonically present, as well as phasically elevated by neuronal activity that results in the release of this, and possibly other endocannabinoids (Freund et al., 2003). Evidence exists for both possibilities in the CNS. For example, the exposure of neurons to chronic ethanol results in an increased accumulation of AEA (Basavarajappa and Hungund, 2002), and chronic ethanol intake increases AEA levels in various brain regions involved in drug abuse (Gonzalez et al., 2004). Thus, alterations in AEA levels in the CNS by abused drugs and/or other pathophysiological conditions may cause changes in tonic activity of nAChRs and/or alter the actions of other abusive substances such as ethanol on nAChR function (Oz et al., 2005). Additionally, our study provides further support for the idea that AEA may tonically inhibit $\alpha4\beta2$ nAChRs, since the effects of exogenously applied

Molecular Pharmacology Fast Forward. Published on July 12, 2007 as DOI: 10.1124/mol.107.036939
This article has not been copyedited and formatted. The final version may differ from this version.

AEA were reversed by lipid scavenging with BSA (Bojesen and Hansen, 2003), and α4β2 nAChR function was increased by BSA in naïve cells. Also consistent with this proposal is the observation that direct manipulation of the membrane lipid composition causes significant alterations in the activity of nicotinic receptors (Baenziger et al., 2000), suggesting that nAChRs do indeed function under the tonic influence of membrane lipids.

In the central nervous system, α4β2 nACh receptors are located both pre- and postsynaptically and play an important modulatory role in synaptic transmission (Sher et al., 2004; Dani and Bertrand, 2007). Because AEA acts at the nAChR at physiologically relevant concentrations (discussed in Oz, 2006) and given the presence of α4β2 nACh receptors in these critical locations, it is possible that the activity of the α4β2-nACh receptor function is regulated by both tonic and phasic AEA in situ. Whereas the α4β2 nACh receptor represents a novel molecular target for AEA, previously observed interactions between Δ^9-THC and systemic nicotinic pharmacology (for reviews see Castane et al., 2006; Viveros et al., 2006) can not be explained by our findings. Other studies indicate that the function of 5-HT_3 and Glycine receptors are also modulated by AEA and by Δ^9-THC (Barann et al., 2002; Oz et al., 2002; Hejazi et al., 2006). However, the present results indicate that AEA, but not Δ^9-THC, inhibits α4β2 nAChR function. Similarly, differential effects of AEA and Δ^9-THC have been reported on Ca^{2+} channels (Oz et al., 2004a), K^+ channels (Poling et al., 1996), α_7-nAChRs (Oz et al., 2004b), and NMDA receptors (Hampson et al., 1998) suggesting that AEA and Δ^9-THC do not share a common binding site among various membrane proteins.

Molecular Pharmacology Fast Forward. Published on July 12, 2007 as DOI: 10.1124/mol.107.036939
This article has not been copyedited and formatted. The final version may differ from this version.

In conclusion, our results indicate that AEA inhibits the function of α4β2 nAChRs and suggest that these receptors may represent a novel target for the actions of AEA in the nervous system.

Molecular Pharmacology Fast Forward. Published on July 12, 2007 as DOI: 10.1124/mol.107.036939
This article has not been copyedited and formatted. The final version may differ from this version.

ACKNOWLDEGEMENTS

The authors wish to thank Dr. Ronald J. Lukas (Barrow Neurological Institute, Phoenix, AZ) for providing the SH-EP1 cell line stably expressing the α4β2 nAChR. We are indebted to Carol Beglan for expert maintenance of the SH-EP1 cell line.

REFERENCES

Akk G, Shu HJ, Wang C, Steinbach JH, Zorumski CF, Covey DF and Mennerick S. (2005) Neurosteroid access to the GABAA receptor. *J Neurosci* **25**:11605-11613.

Baenziger J E, Morris ML, Darsaut TE and Ryan SE (2000) Effect of membrane lipid composition on the conformational equilibria of the nicotinic acetylcholine receptor. *J Biol Chem* **275**: 777-784.

Barann M, Molderings G, Bruss M, Bonisch H, Urban BW and Gothert M (2002) Direct inhibition by cannabinoids of human 5-HT3A receptors: probable involvement of an allosteric modulatory site. *Br J Pharmacol* **137**:589-596.

Barrantes FJ (2004) Structural basis for lipid modulation of nicotinic acetylcholine receptor function. *Brain Res Brain Res Rev* **47**: 71-95.

Basavarajappa BS and Hungund BL (2002) Neuromodulatory role of the endocannabinoid signaling system in alcoholism: an overview. *Prostaglandins Leukot Essent Fatty Acids* **66:**287-299.

Bojesen, IN and Hansen HS (2003) Binding of anandamide to bovine serum albumin. *J Lipid Res* **44**: 1790-1794.

Bojesen IN and Hansen HS (2006) Effect of an unstirred layer on the membrane permeability of anandamide. *J Lipid Res* **47**: 561-570.

Brody AL, Mandelkern MA, London ED, Olmstead RE, Farahi J, Scheibal D, Jou J, Allen V, Tiongson E, Chefer SI, Koren AO and Mukhin AG (2006) Cigarette smoking saturates brain alpha 4 beta 2 nicotinic acetylcholine receptors. *Arch Gen Psychiatry* **63**: 907-915.

Castane A, Berrendero F and Maldonado R (2005) The role of the cannabinoid system in nicotine addiction. *Pharmacol Biochem Behav* **8**:381-386.

Chemin J, Monteil A, Perez-Reyes E, Nargeot J and Lory P (2001) Direct inhibition of T-type calcium channels by the endogenous cannabinoid anandamide. *EMBO J* **20**:7033-7040.

Dani JA and Bertrand D (2007) Nicotinic Acetylcholine Receptors and Nicotinic Cholinergic Mechanisms of the Central Nervous System. *Annu Rev Pharmacol Toxicol* **47**:699-6729.

Ellena JF, Blazing MA and McNamee MG (1983) Lipid-protein interactions in reconstituted membranes containing acetylcholine receptor. *Biochemistry* **22**: 5523-5535.

Fenster CP, Beckman ML, Parker JC, Sheffield EB, Whitworth TL, Quick MW and Lester RA (1999) Regulation of alpha4beta2 nicotinic receptor desensitization by calcium and protein kinase C. *Mol Pharmacol* **55**: 432-443.

Fisyunov A, Tsintsadze V, Min R, Burnashev N and Lozovaya NA (2006) Cannabinoids modulate the P-type high voltage-activated calcium currents in Purkinje neurons. *J Neurophysiol* **96**: 1267-1277.

Freund TF, Katona I and Piomelli D (2003) Role of endogenous cannabinoids in synaptic signaling. *Physiol Rev* **83**:1017-1066.

Fucile S (2004) Ca2+ permeability of nicotinic acetylcholine receptors. *Cell Calcium* **35**:1-8.

Gonzalez S, Valenti M, de Miguel R, Fezza F, Fernandez-Ruiz J, Di Marzo V and Ramos JA (2004) Changes in endocannabinoid contents in reward-related brain regions of alcohol-exposed rats, and their possible relevance to alcohol relapse. *Br J Pharmacol*

143:455-464.

Hampson AJ, Bornheim LM, Scanziani M, Yost CS, Gray AT, Hansen BM, Leonoudakis DJ and Bickler PE (1998) Dual effects of anandamide on NMDA receptor-mediated responses and neurotransmission. *J Neurochem* **70**:671-676.

Hejazi N, Zhou C, Oz M, Sun H, Ye JH and Zhang L (2006) Delta9-tetrahydrocannabinol and endogenous cannabinoid anandamide directly potentiate the function of glycine receptors. *Mol Pharmacol* **69**:991-997.

Howlett AC, Barth F, Bonner TI, Cabral G, Casellas P, Devane WA, Felder CC, Herkenham M, Mackie K, Martin BR, Mechoulam R and Pertwee RG (2002) International Union of Pharmacology. XXVII. Classification of cannabinoid receptors. *Pharmacol Rev* **54**:161-202.

Kamp F and Hamilton JA (1993) Movement of fatty acids, fatty acid analogues, and bile acids across phospholipid bilayers. *Biochemistry* **32**:11074-11086.

Kathuria S, Gaetani S, Fegley D, Valino F, Duranti A, Tontini A, Mor M, Tarzia G, La Rana G, Calignano A, Giustino A, Tattoli M, Palmery M, Cuomo V and Piomelli D (2003) Modulation of anxiety through blockade of anandamide hydrolysis. *Nat Med* **9**:76-81.

Lambert DG, Ghataorre AS and Nahorski SR (1989) Muscarinic receptor binding characteristics of a human neuroblastoma SK-N-SH and its clones SH-SY5Y and SH-EP1. *Eur J Pharmacol* **165**:71-77.

Laviolette SR and van der Kooy D (2004) The neurobiology of nicotine addiction: bridging the gap from molecules to behaviour. *Nat Rev Neurosci* **5**:55-65.

Lundbaek JA (2006) Regulation of membrane protein function by lipid bilayer elasticity - a single molecule technology to measure the bilayer properties experienced by an embedded protein. *Journal of Physics-Condensed Matter* **18**:S1305-S1344.

Murase K, Ryu PD and Randic M (1989) Excitatory and inhibitory amino acids and peptide-induced responses in acutely isolated rat spinal dorsal horn neurons. *Neurosci Lett* **103**:56-63.

Nicholson RA, Liao C, Zheng J, David LS, Coyne L, Errington AC, Singh G and Lees G (2003) Sodium channel inhibition by anandamide and synthetic cannabimimetics in brain. *Brain Res* **978**:194-204.

Oliver D, Lien CC, Soom M, Baukrowitz T, Jonas P and Fakler B (2004) Functional conversion between A-type and delayed rectifier K+ channels by membrane lipids. *Science* **304**: 265-270.

Oz M (2006) Receptor-independent actions of cannabinoids on cell membranes: focus on endocannabinoids. *Pharmacol Ther* **111**:114-144.

Oz M, Tchugunova YB and Dunn SM (2000) Endogenous cannabinoid anandamide directly inhibits voltage-dependent Ca(2+) fluxes in rabbit T-tubule membranes. *Eur J Pharmacol* **404**:13-20.

Oz M, Zhang L and Morales M (2002) Endogenous cannabinoid, anandamide acts as a non-competitive inhibitor on 5-HT_3 receptor-mediated responses in *Xenopus* oocytes. *Synapse* **46**: 150-156.

Oz M, Ravindran R, Zhang L and Morales M (2003) Endogenous cannabinoid, anandamide inhibits neuronal nicotinic acethylcholine receptor-mediated responses in *Xenopus* oocytes. *J Pharmacol Exp Ther* **306**: 1003-1010.

Oz M, Tchugunova Y and Dinc M (2004a) Differential Effects of Endocannabinoids and Synthetic Cannabinoids on Voltage-Dependent Calcium Fluxes in Rabbit T-Tubule Membranes; Comparison With Fatty Acids. *Eur J Pharmacol* **502:** 47-58.

Oz M, Ravindran R, Zhang L, Morales M and Lupica CR (2004b) Direct and differential effects of cannabinoid receptor ligands on α_7-nicotinic receptor-mediated currents in *Xenopus* oocytes. *J Pharmacol Exp Ther* **310**: 1152-1160.

Oz M, Jackson S, Woods A, Morales M and Zhang L (2005) Additive effects of endogenous cannabinoid anandamide and ethanol on alpha7-nicotinic acetylcholine receptor-mediated responses in Xenopus oocytes. *J Pharmacol Exp Ther* **313**: 1272-1280.

Pacheco MA, Pastoor TE, Lukas RJ and Wecker L (2001) Characterization of human alpha4beta2 neuronal nicotinic receptors stably expressed in SH-EP1 cells. *Neurochem. Res*. **26**:683-693.

Pacher P, Batkai S and Kunos G (2006) The endocannabinoid system as an emerging target of pharmacotherapy. *Pharmacol Rev* **58**: 389-462.

Paradiso KG and Steinbach JH (2003) Nicotine is highly effective at producing desensitization of rat alpha4beta2 neuronal nicotinic receptors. *J Physiol* **553**:857-871.

Poling JS, Rogawski MA, Salem N and Vicini S (1996) Anandamide, an endogenous cannabinoid inhibits Shaker-related voltage-gated K+ channels. *Neuropharmacology* **35**:983-991.

Quick MW and Lester RA (2002) Desensitization of neuronal nicotinic receptors. *J Neurobiol* **53**:457-478.

Sher E, Chen Y, Sharples TJ, Broad LM, Benedetti G, Zwart R, McPhie GI, Pearson KH, Baldwinson T and De Filippi G (2004) Physiological roles of neuronal nicotinic receptor subtypes: new insights on the nicotinic modulation of neurotransmitter release, synaptic transmission and plasticity. *Curr Top Med Chem* **4**: 283-297.

Spivak CE, Oz M, Beglan CL and Shrager RI (2006) Diffusion delays and unstirred layer effects at monolayer cultures of Chinese hamster ovary cells: radioligand binding, confocal microscopy, and mathematical simulations. *Cell Biochem Biophys* **45**: 43-58.

Tapper AR, McKinney SL, Nashmi R, Schwarz J, Deshpande P, Labarca C, Whiteaker P, Marks MJ, Collins AC and Lester HA (2004) Nicotine activation of alpha4* receptors: sufficient for reward, tolerance, and sensitization. *Science* **306**: 1029-1032.

Wu J, Kuo YP, George AA, Xu L, Hu J and Lukas RJ (2004) beta-Amyloid directly inhibits human alpha4beta2-nicotinic acetylcholine receptors heterologously expressed in human SH-EP1 cells. *J Biol Chem* **279**: 37842-37851.

Viveros MP, Marco EM, and File SE (2006) Nicotine and cannabinoids: Parallels, contrasts and interactions. *Neurosci Biobehav Rev* **30**: 1161-1181.

Molecular Pharmacology Fast Forward. Published on July 12, 2007 as DOI: 10.1124/mol.107.036939
This article has not been copyedited and formatted. The final version may differ from this version.

FOOTNOTES

This study was supported by funds from the Intramural Research Program of the National Institute on Drug Abuse, U.S. Department of Health and Human Services.

Molecular Pharmacology Fast Forward. Published on July 12, 2007 as DOI: 10.1124/mol.107.036939
This article has not been copyedited and formatted. The final version may differ from this version.

FIGURE LEGENDS

Scheme 1. Kinetic scheme showing the agonist-bound and activated (conducting) nAChR, denoted AR*, sequentially converting to desensitized states AR' and AR" by the first order forward and backward rate constants k_1, k_{-1} and k_2, k_{-2}, respectively.

1. Peak amplitudes, normalized to the maximum observed for each cell, are shown plotted as a function of the ACh concentration at the SH-EP1 cells stably expressing the α4β2 nAChR. The cells were voltage clamped to -60 mV using the whole cell technique. Means ± s.e.m. are shown. The left inset shows typical current traces in a single cell at various concentration of ACh, and the right inset shows the decomposition of the response to 100 μM ACh into its two exponential components.

2. Kinetics of desensitization as a function of the ACh concentration. The decays of the responses to ACh were analyzed according to the model of two sequential states denoted by Scheme 1 to yield the four rate constants. Panels A, C, E, and F plot the four rate constants as functions of the ACh concentration. Panels B and D are scatter plots of the peak amplitudes vs. forward rate constants $k_1$and k_2, respectively. Symbols represent means ± s.e m.

3. The effects of AEA on responses to 30 μM ACh. Panel A shows representative responses of a cell under control condition followed by continuous superfusion of 1 μM AEA for 3 and 40 min. In B, normalized peak amplitudes are plotted as a function of

Molecular Pharmacology Fast Forward. Published on July 12, 2007 as DOI: 10.1124/mol.107.036939
This article has not been copyedited and formatted. The final version may differ from this version.

time and concentration of AEA. In this and subsequent panels, filled squares (■) represent the control condition; filled circles (●), 200 nM AEA; open squares (□), 500 nM AEA; filled triangles (▲) and X symbols (at 6 min intervals), 1 μM AEA; and open circles (○), 2 μM AEA. The desensitization rate constants are shown plotted as a function of time in panels C, E, F, and G. Asymptotes of the k_1 values, taken from C, are plotted as a function of the AEA concentration in D with uncertainties obtained from fitting the curves in C to an exponential function.

4. Representative traces for responses of a cell to 30 μM ACh under control condition, after 14 min of continuous superfusion of 1 μM Δ^9-THC, and after the washout of the Δ^9-THC.

5. Effects of 1 μM SR-141716A on peak amplitudes and desensitization rate constants on responses to 30 μM ACh in the continuous presence of 1 μM AEA. Squares represent control values (with AEA but in the absence of SR-141716A), and circles represent values obtained in the presence of SR-141716A. Symbols represent means ± s.e.m.

6. Lipid-free bovine serum albumin (BSA) accelerated the recovery from AEA treatment. The effects on peak amplitudes and desensitization rate constant k_1 are shown in left and right columns, respectively. A and B show the control condition, in which cells were treated with AEA (1 μM) for 3 min (first vertical dotted line) immediately prior to the wash denoted as time = 0 (second dotted line). The dashed line in A

represents the rundown of peak amplitudes under AEA-free conditions taken from the dashed line in Fig. 3B. C and D show similar experiments in which the cells were treated with AEA for 10 min followed by wash with medium containing BSA at 1 mg/mL.

7. Effects of BSA (1 mg/mL) on naive cells. The effects of BSA on peak amplitudes (A) and desensitization rate constant k_1 are shown in A and B, respectively.

8. Hypothetical potential energy vs. reaction coordinate plot showing the energies of the activated receptor AR*, the transition state, and the first desensitized state AR' (see Scheme 1) under the control condition (solid curve) and conditions in which the activation energy is reduced (dotted curve) and in which the energy of the activated state is raised (dashed curve). Only the latter alternative would solely increase k_1.

$$AR^* \underset{k_{-1}}{\overset{k_1}{\rightleftharpoons}} AR' \underset{k_{-2}}{\overset{k_2}{\rightleftharpoons}} AR''$$

Scheme 1

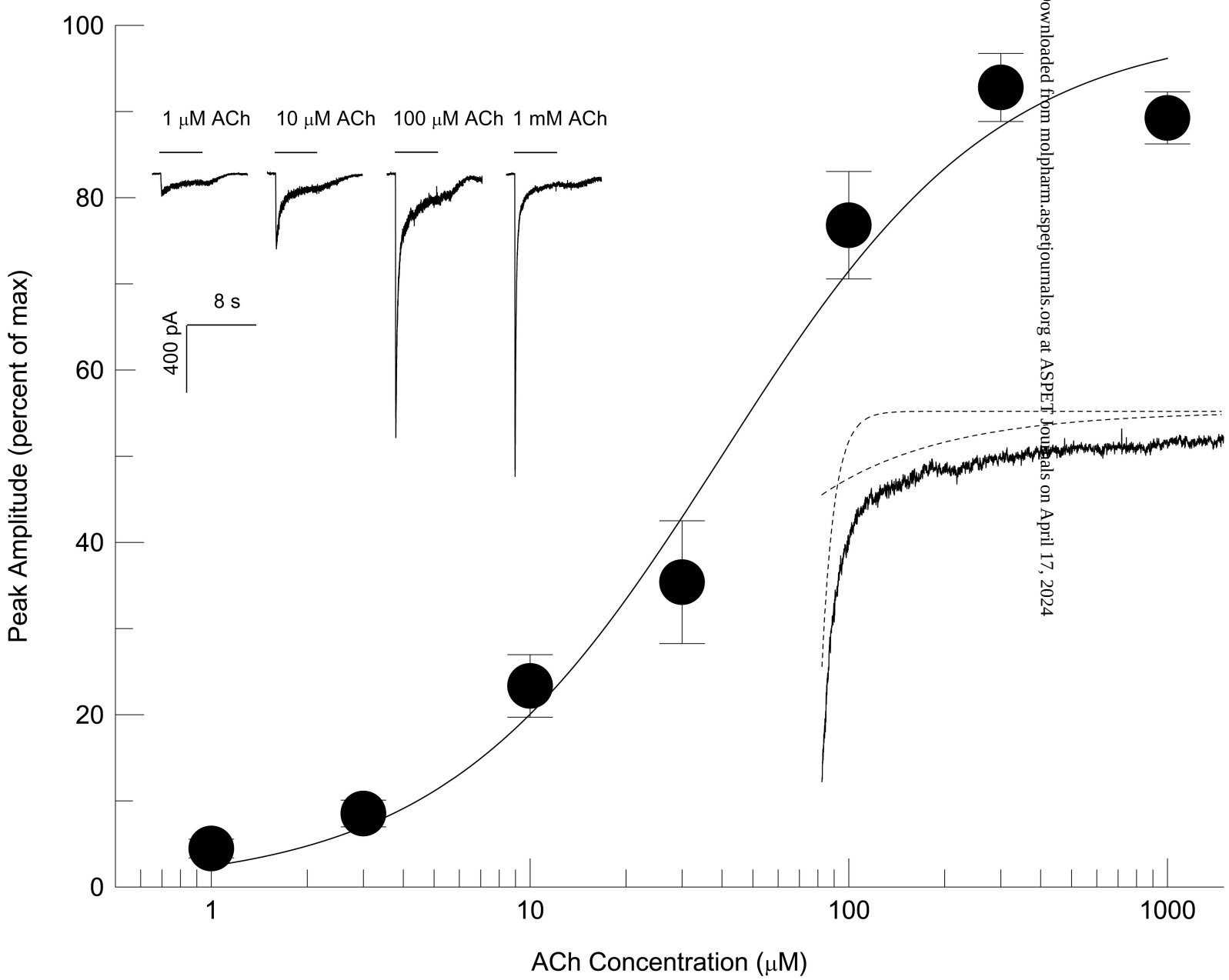

Figure 1

Molecular Pharmacology Fast Forward. Published on July 12, 2007 as DOI: 10.1124/mol.107.036939
This article has not been copyedited and formatted. The final version may differ from this version.

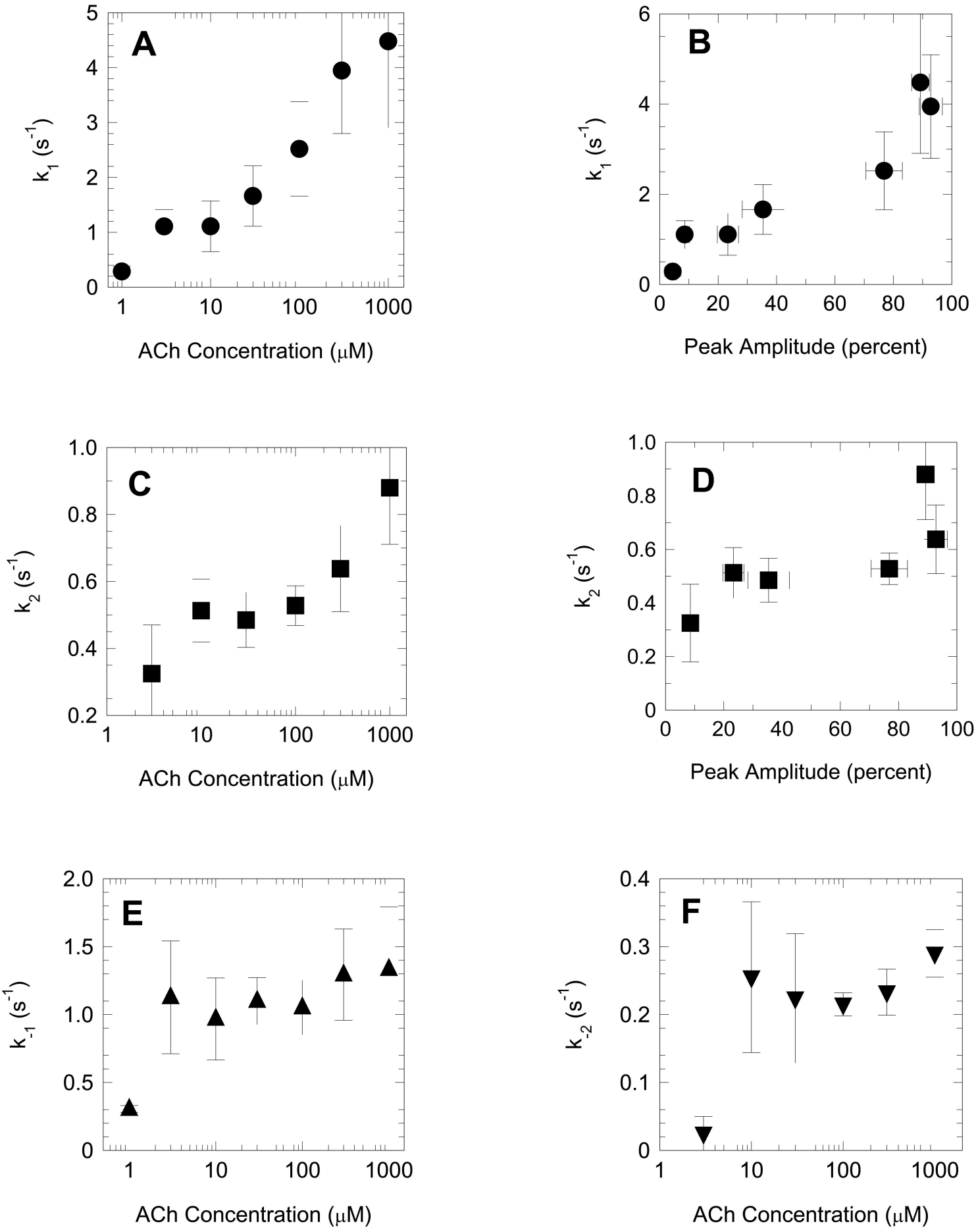

Figure 2

Molecular Pharmacology Fast Forward. Published on July 12, 2007 as DOI: 10.1124/mol.107.036939
This article has not been copyedited and formatted. The final version may differ from this version.

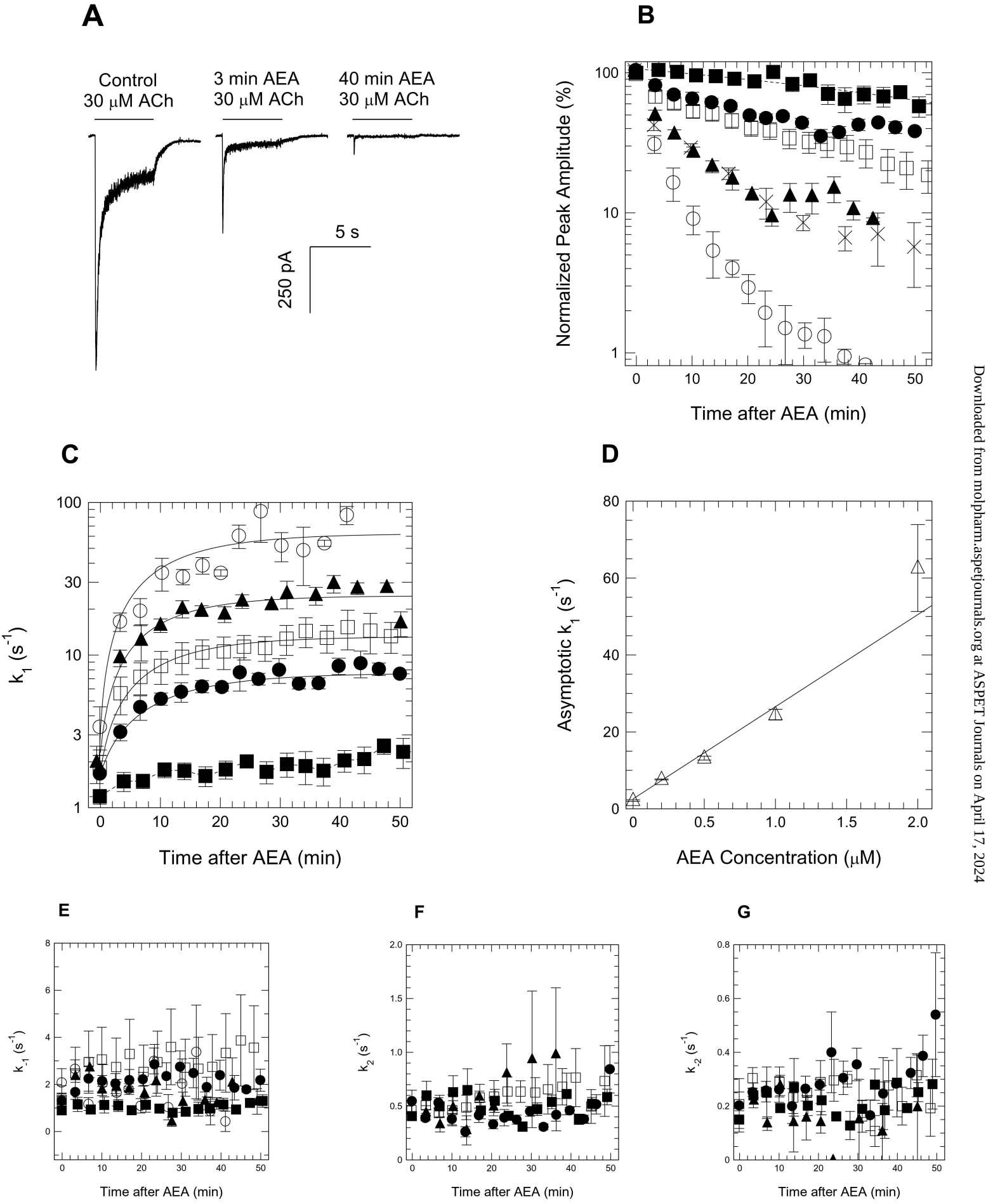

Figure 3

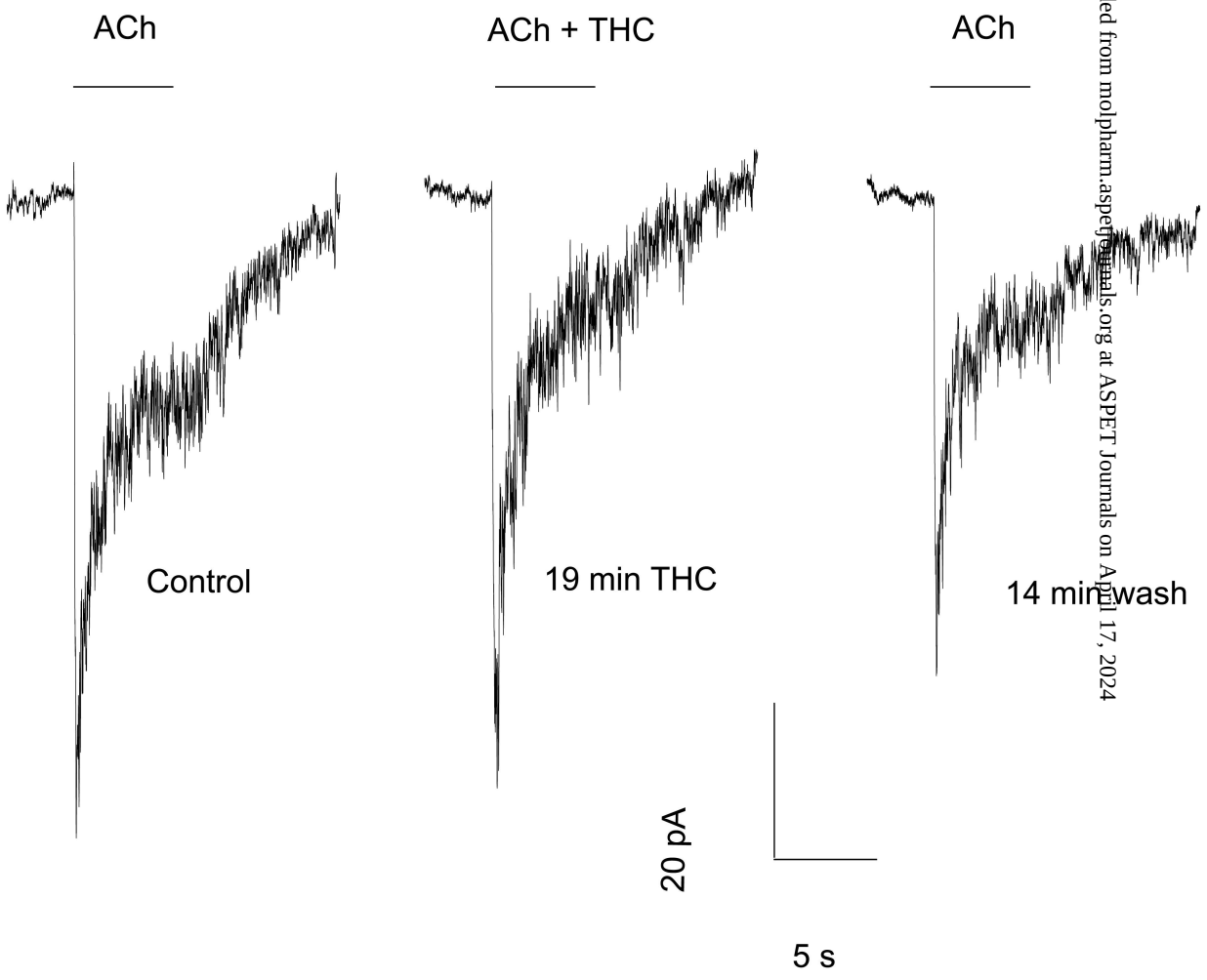

Figure 4

Molecular Pharmacology Fast Forward. Published on July 12, 2007 as DOI: 10.1124/mol.107.036939
This article has not been copyedited and formatted. The final version may differ from this version.

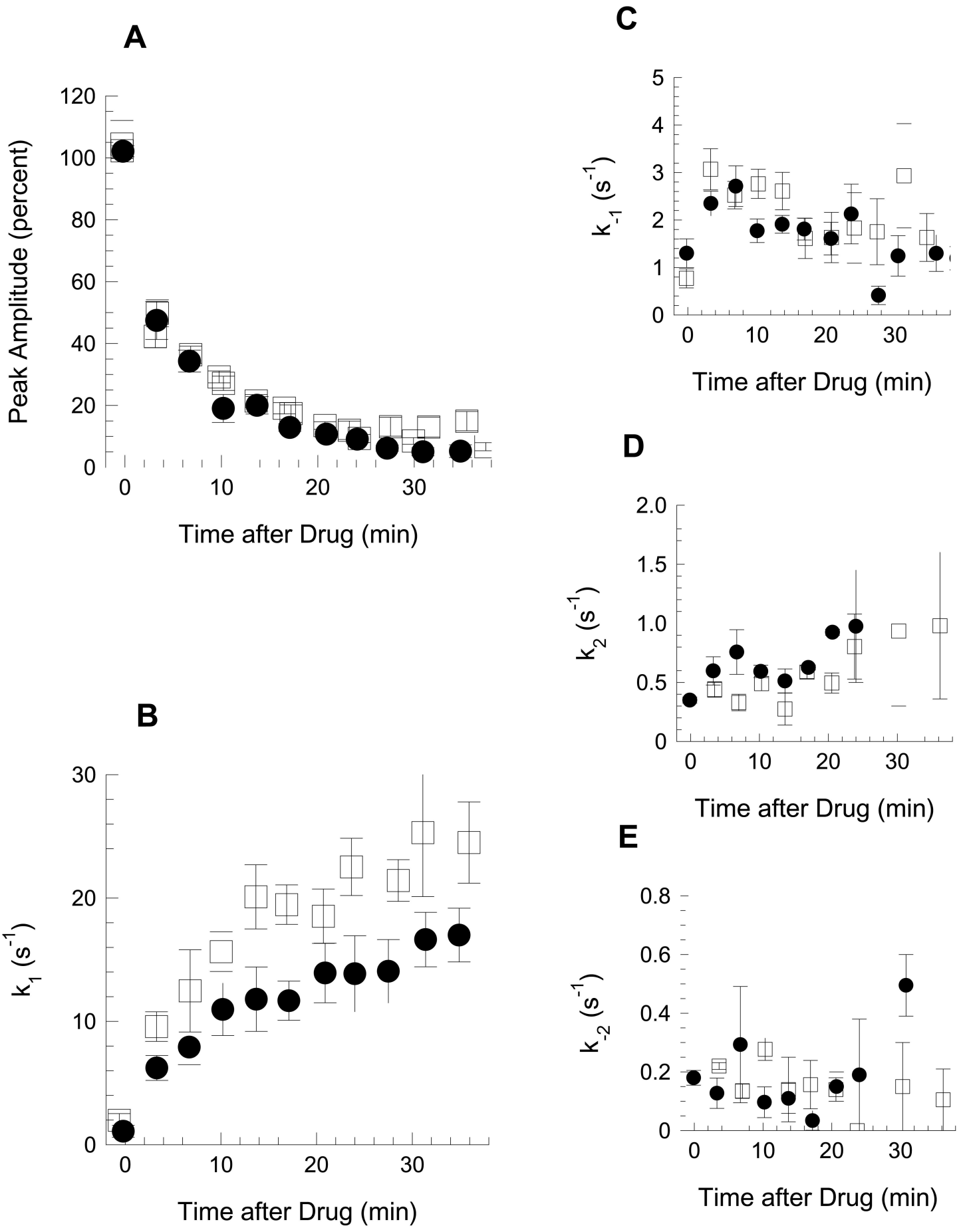

Figure 5

Molecular Pharmacology Fast Forward. Published on July 12, 2007 as DOI: 10.1124/mol.107.036939
This article has not been copyedited and formatted. The final version may differ from this version.

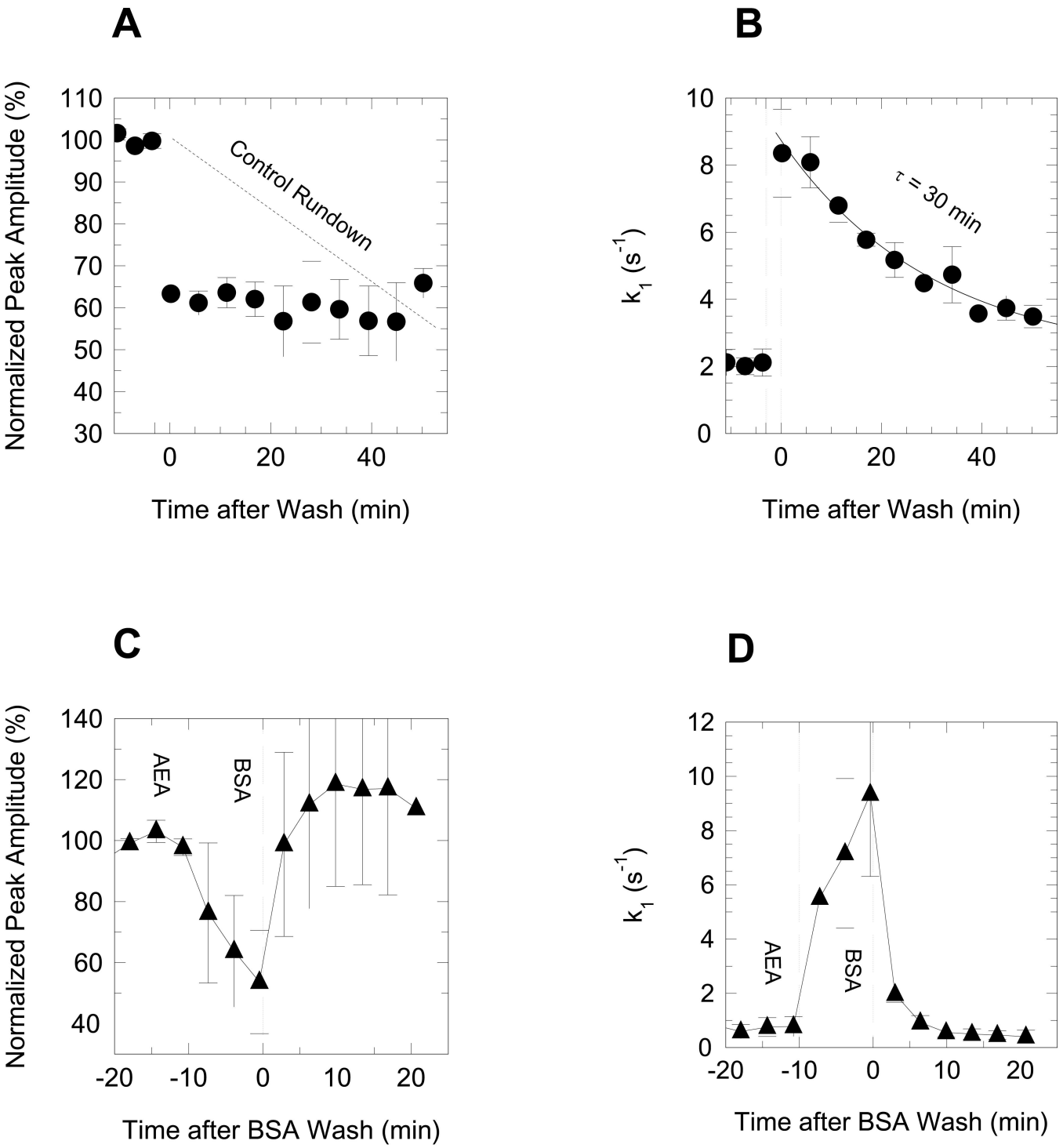

Figure 6

Molecular Pharmacology Fast Forward. Published on July 12, 2007 as DOI: 10.1124/mol.107.036939
This article has not been copyedited and formatted. The final version may differ from this version.

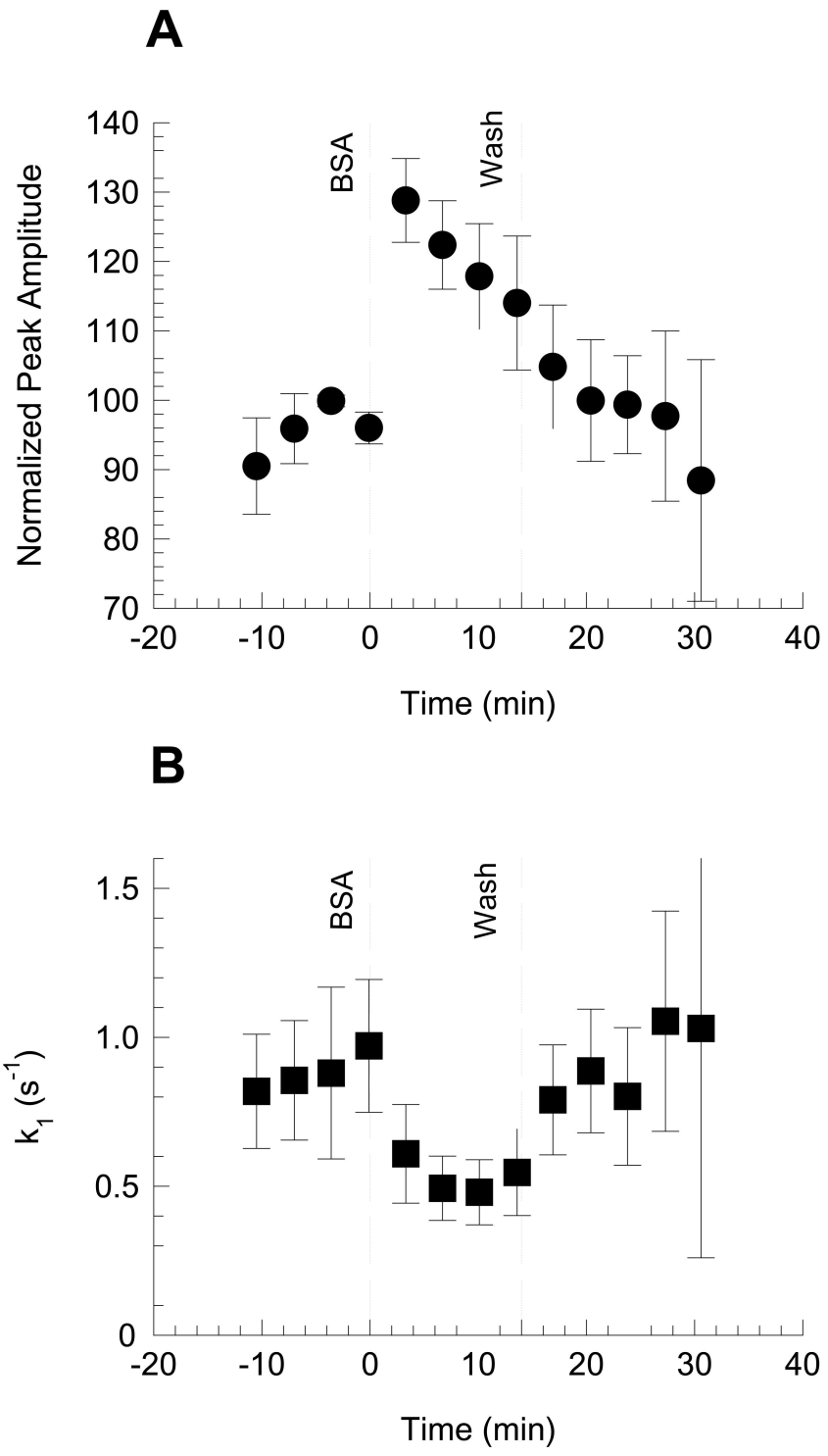

Figure 7

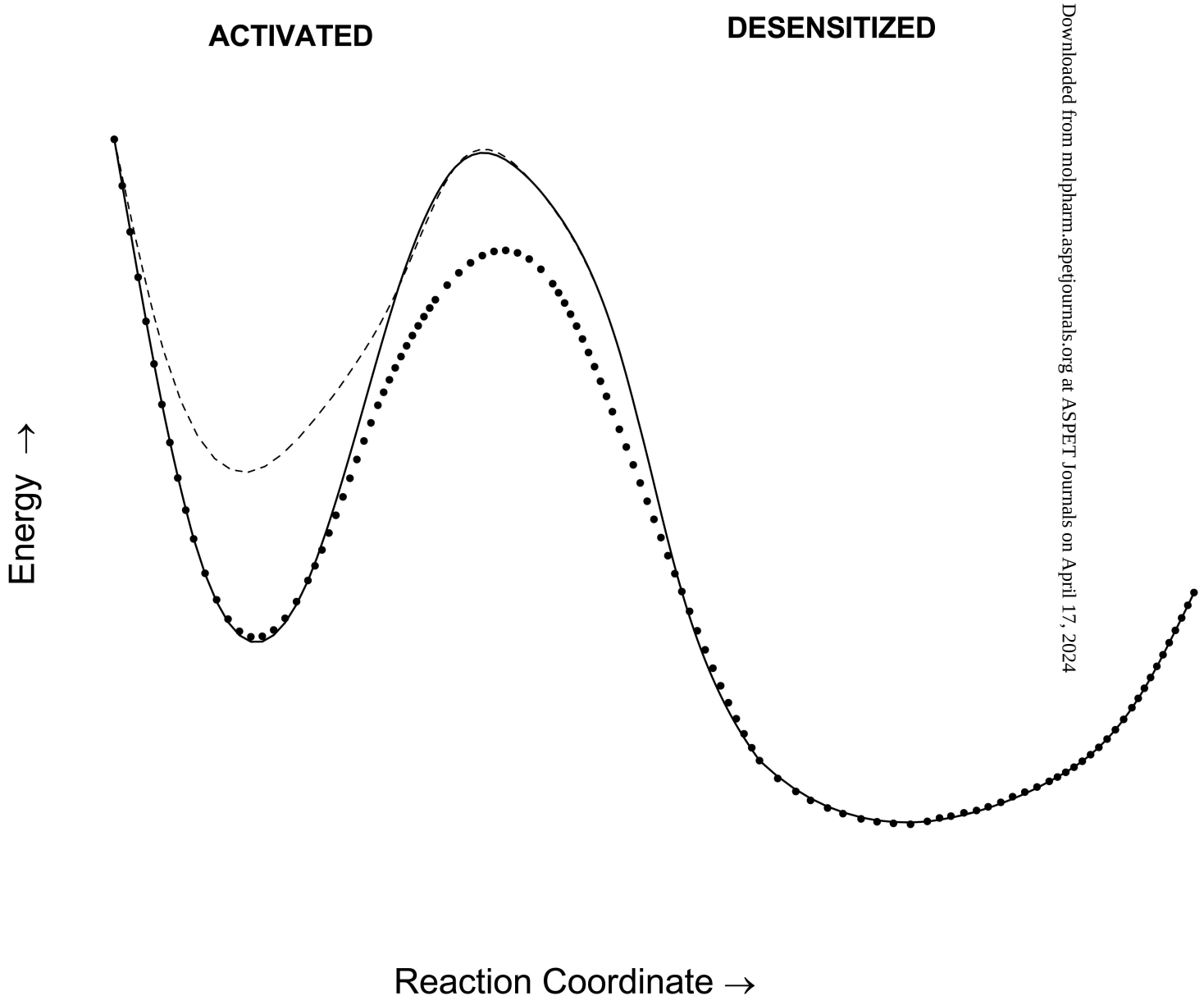

Figure 8

Supplemental Material

I. Diminution of peak amplitudes by rapid desensitization.

The initial activation of the nAChR is a multi-step process that consists of the convective flow of ACh solution from the superfusing pipette, the diffusion of ACh through an unstirred layer, and an activation sequence consisting of ligand binding and the receptor conformation change.

The elementary response.

Details of many of these steps are not known in reliable, quantitative detail and are not critical to the argument here, so we empirically model the rising phase of the ACh response at a single point on the cell surface as the elementary function $AR^*(t) = \tanh(\theta^*t)$. This function with $\theta=200\ s^{-1}$ gives a 10 - 90% rise time of 6.9 ms. This well-behaved function has the simplicity and tractability for easy use in the differential equations for receptor activation and desensitization. Using the two stage desensitization mechanism embodied in Scheme 1 of the text and rate constants for the control condition of $k_1 = 1.5\ s^{-1}$, $k_{-1} = 1.0\ s^{-1}$, $k_2 = 0.5\ s^{-1}$, and $k_{-2} = 0.2\ s^{-1}$, the simulated activation-desensitization time course curve is as follows:

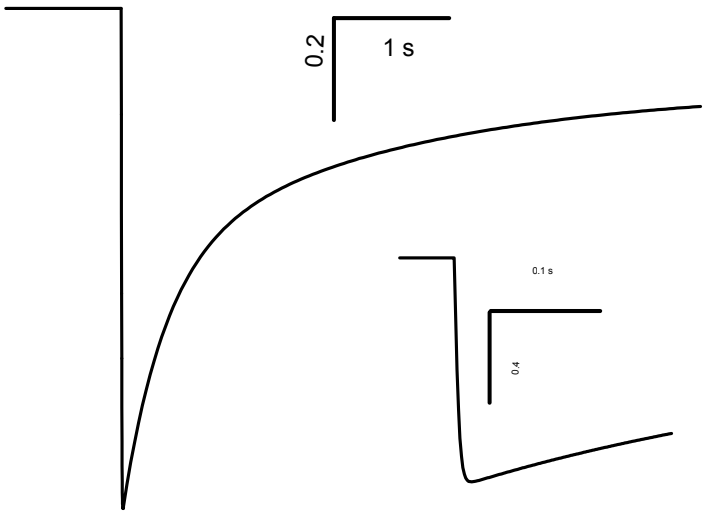

Five seconds of simulated decay are shown in the main plot, and 0.2 s are shown in the inset.

The effect of increasing the first stage forward rate constant for desensitization,

k_1 as in the presence of AEA, is shown in the following simulations:

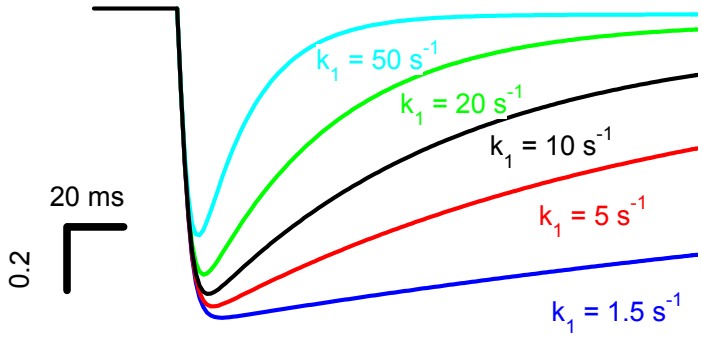

There is a 28% decrease in peak amplitude just due to a k_1 value that has increased to 50 s^{-1} while the rise time remains at < 7 ms.

The effect of changing the rise time (through the parameter θ) of the elementary response above on the peak amplitudes both when k_1 = 1.5 s^{-1} (control) and k_1 = 50 s^{-1} is depicted in the graph below. When the rise time is 70 ms and k_1 = 50 s^{-1}, the peak amplitude is 22% of the maximum. The simulated currents under these conditions are shown as the inset.

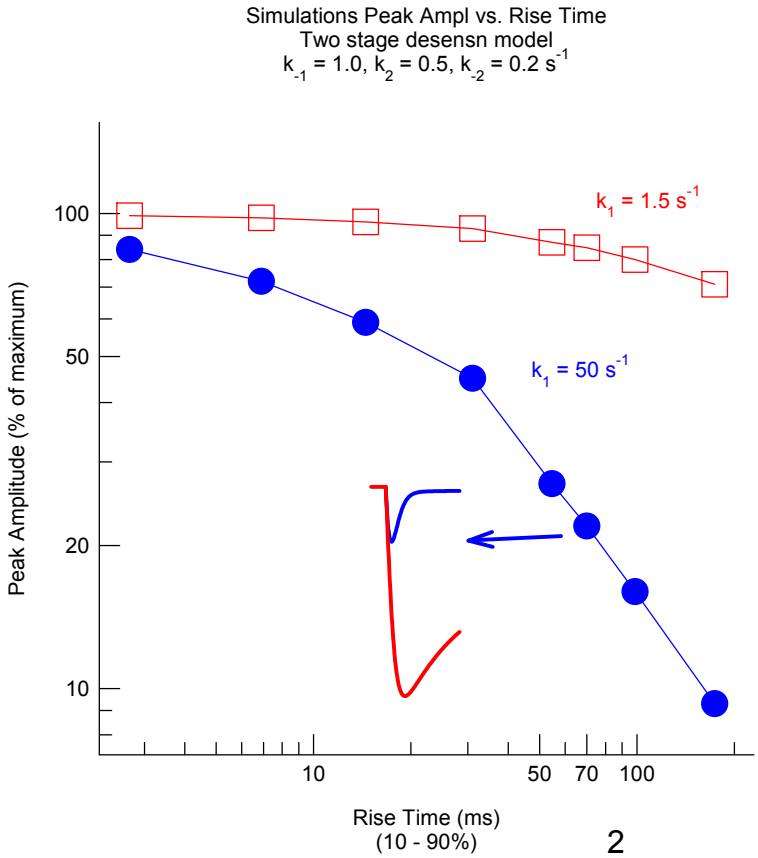

The summated response.

The model: Receptors are dispersed over the surface of the cell, depicted as dots in the figure below. The jet of agonist solution (red) directed at the cell at the bottom of the culture dish is deflected by an unstirred layer through which the ACh diffuses passively. Given diffusion dimensions of ~ 10 μm and a diffusion coefficient of 9.8 x 10^{-6} cm^2s^{-1} (1), the diffusion-limited rise time for the ACh to reach its nominal pipette concentration over the entire surface of the cell is on the order of ~ 50 ms. As shown in the figure, during that access time, receptors activated first could already be desensitzed (black dots) while others (green dots) are activated and more distant ones (yellow dots) are still unactivated. The recorded signal is the summation of all the receptors activated at any time.

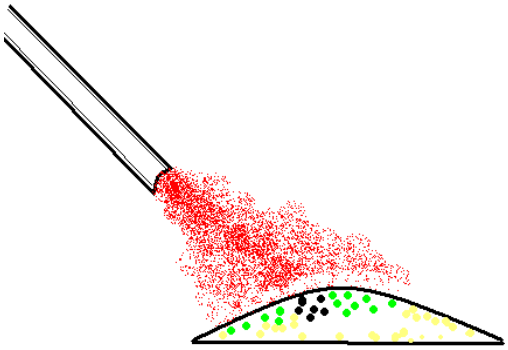

The simulations:

Assume that the measured response is the sum of elementary responses described on p.1 with rise times of 6.9 ms and that the wave of ACh reaches the receptors as a Gaussian function of time with a standard deviation of 50 ms (and mean of 120 ms). The figure at the left below shows how nine such elementary responses sum when k_1 = 1.5 s^{-1} (control), and at the right when k_1 = 50 s^{-1}.

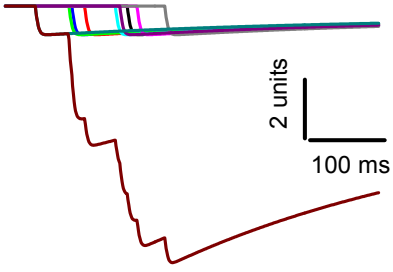

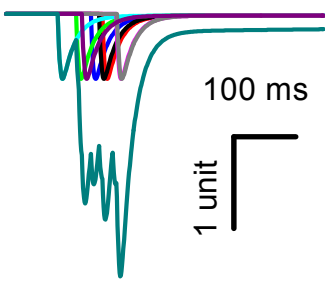

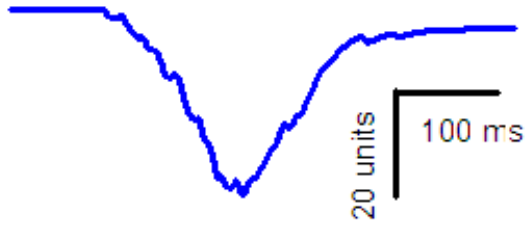

Notice that when $k_1 = 1.5\ s^{-1}$ the 9 elementary responses sum to 8.7, but that when $k_1 = 50\ s^{-1}$ they sum to only 2.9 units because desensitization is so rapid that the superposition approaches a sequence of unitary responses. Summating 200 such responses ($k_1 = 50\ s^{-1}$) gives the curve at the left, with a peak of about 35 units, i.e. 18% of the summated peak when there is no desensitization.

If, instead of simply summing discrete elementary units, one convolves the response curve with a Gaussian function using a range of standard deviations, one obtains the series of curves below. The non-desensitized maximum in this plot is unity. Note that peak amplitudes decrease with increasing rise time, but that the decays become distorted at rise times slower than about 50 ms. At this and slower rise times, the entire signal becomes an imitation of the Gaussian activation wave.

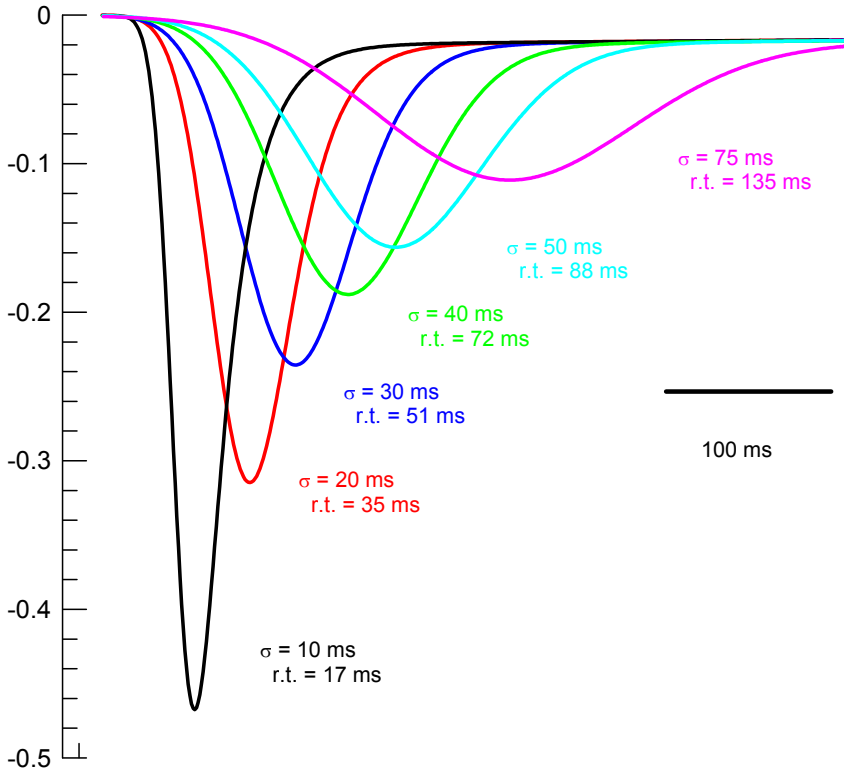

Summary and conclusions

1. An elementary response function that neglects the lateral dispersion of receptors on a cell shows that the peak response is diminished when the desensitization rate constant k_1 increases. When $k_1 = 50\ s^{-1}$ and the rise time is ~ 100 ms, the peak amplitude is diminished to about 15% of the control value.

2. Simulating lateral spread of the activation by summing elementary response functions over a Gaussian distribution in time shows that peak amplitudes diminish as rise time increases, but at rise times >50 ms, the decays become governed by the spread of activation rather than the kinetics of desensitization. The peak amplitude at this threshold is about 20% of the maximum. Activation waves that are skewed Gaussians would give slightly different results. As the rate constants we measured at 2 μM AEA were generally consistent with those at lower concentrations, we believe that distortions of the decays by the activation wave were not evident in our experiments.

3. In these ways, one can easily account for diminutions in peak amplitude of up to about 80% by the increase in the desensitization rate constant k_1 that resulted from the treatment with AEA. Greater diminution, such as the 99% block seen in 2 μM AEA, are not as readily accounted for by this model because they require unrealistically slow rise times and distortion of the decay phase that was not experimentally apparent. We therefore consider other mechanisms of current block, of which desensitization of the closed channel seems most parsimonious.

II. Deriving rate constants from the decay curves: a stepwise explication.

For this discussion, we neglect the diffusion of ACh to receptors, described in part I above, and assume that it is instantaneous contact with a homogeneous population of about 1000 receptors (based on a maximum current of 2 nA and taking a single channel conductance — estimates vary from 13 to 46 pS — as 30 pS, and a holding potential of -60 mV). Neglecting desensitization and open channel block by the agonist, each receptor undergoes cycles of states from inactive to occupation by the agonist to activation (open channel) and back over a time scale of about a millisecond (e.g. see Maconochie and Steinbach (1998)). Therefore, the activation state of this population of channels can be considered to be in equilibrium with the agonist at the time scale of desensitization, which (even in the presence of AEA) is at about two or more orders of magnitude slower. Because of this equilibrium, we can consider the activated state, AR*, as a single entity without regard to the activation steps.

We now consider the simplest case for desensitization, when the decay of the peak current occurs by a single exponential decay. The corresponding kinetic scheme is as follows:

$$AR^* \underset{k_{-1}}{\overset{k_1}{\rightleftarrows}} AR'$$

where AR' is a non-conducting, desensitized state. This scheme says that the population of activated receptors, AR*, is diminished at a rate equal to the concentration of AR* times the rate constant k_1. As AR* becomes depleted by being transformed to AR', the rate decreases, so a plot of the remaining AR* (indicated by current that is monitored by whole cell patch clamp) follows an exponential time course. AR* would diminish to zero were it not for the recovery from desensitization represented by the backward arrow in the scheme above. This recovery limits the final extent of desensitization so that AR* levels off to an asymptote level, a direct measure of its presence. The time course and the asymptote are determined completely by the rate constants k_1 and k_{-1} as solutions of the corresponding differential equation:

$$d[AR^*]/dt = - k_1 [AR^*] + k_{-1} [AR']$$

[AR'] is not observed directly, but the peak activation, $[AR^*_0]$ (the initial condition), is observed, so the equation can be expressed to account for the conservation of receptors as

$$d[AR^*]/dt = - k_1 [AR^*] + k_{-1} ([AR^*_0] - [AR^*])$$

or

$$d[AR^*]/dt = -(k_{-1} + k_1)[AR^*] + k_{-1}[AR^*_0]$$

where $[AR^*_0]$ is a constant through time. This differential equation can be solved by the separation of variables method, which yields the following integrated rate equation:

$$[AR^*] = \frac{[AR^*_0] \{k_1 \exp(-(k_1 + k_{-1})t) + k_{-1} \}}{k_1 + k_{-1}}$$

This equation describes a curve that starts at $[AR^*_0]$ when t = 0 and decays with a time constant tau = $1/(k_1 + k_{-1})$ to an asymptote = $[AR^*_0] k_{-1} / (k_1 + k_{-1})$. It shows that when k_{-1} =0, the asymptote is zero; that when $k_{-1} = k_1$ the asymptote is half of

the maximum; and that when $k_{-1} >> k_1$, the decay is imperceptible.

Thus, by fitting the decay curve to an exponential curve with an asymptote to obtain tau and the asymptote, all of the information to convert these two parameters to the two rate constants is obtained.

For the two sequential desensitized states incorporated as Scheme 1, another more complicated function is obtained that describes a double exponential decay to an asymptote. The two time constants, the fraction of each exponential function, and the asymptote are, as in the single exponential case above, convertible to the four rate constants.

References

1. Krnjevic K and Mitchell JF 1960 Diffusion of acetylcholine in agar gels and in the isolated rat diaphragm. *J Physiol*. 153:562-572.

2. Kenneth A. Connors (1990) **Chemical kinetics: The Study of Reaction Rates in Solution**, VCH Publishers, Inc.

3. Maconochie DJ, Steinbach JH.(1998) The channel opening rate of adult- and fetal-type mouse muscle nicotinic receptors activated by acetylcholine. J. Physiol. (Lond.).506:53-72.